

Supplementary Material

Maturation experiments reveal bias in the chemistry of fossil melanosomes

Valentina Rossi¹, Samuel Webb² and Maria McNamara¹

¹*School of Biological, Earth and Environmental Sciences, University College Cork, North Mall, Cork T23 TK30, Ireland.*

²*Stanford Synchrotron Radiation Lightsource (SSRL), SLAC National Accelerator Laboratory, Menlo Park, CA 94025, USA.*

Corresponding authors: valentina.rossi@ucc.ie; maria.mcnamara@ucc.ie

SUPPLEMENTARY METHODS

Enzymatic melanin extraction

The entire liver and 200 mm² samples of skin were dissected from a specimen of the African clawed frog (*Xenopus laevis*) using sterile tools. Melanin was extracted from these tissues using the protocol in Rossi et al. (2019); in brief, samples were treated with nine cycles of solutions containing 1,4-dithiothreitol (DTT), proteinase-K and papain while incubated at 37.5°C at 200 rpm for nine days. Melanin extracts were then washed with biomolecular grade water and acetone and left to dry. This study used three replicates of each tissue for each treatment.

Micro-Synchrotron Rapid Scanning-X-Ray Fluorescence (micro-SRS-XRF)

The incident X-ray energy was set to 11 keV using a Si (111) double crystal monochromator with the storage ring containing 500 mA in top off mode at 3.0 GeV. A microfocused beam of 2 x 2 µm was provided by a Rh-coated Kirkpatrick-Baez mirror pair. The incident X-ray intensity was measured with a nitrogen-filled ion chamber. Samples were mounted at 45° to the incident X-ray beam and were spatially rastered at 50 ms / pixel dwell time with a pixel size of 30 µm x 30 µm.

Fluorescence intensities were corrected and normalized for detector deadtime and variation in I₀ to allow comparison among samples. The concentrations of each element in µg/cm² were calibrated using NIST traceable thin film elemental standards. Micro-SRS-XRF concentration data plus mean and standard deviation data for each element analyzed are listed in Supplementary Data 1 and 2. Loadings from the linear discriminant analysis (LDA) are listed in Supplementary Data 3.

All peaks were fitted using spectrometer zero, spectrometer gain, and detector width in order to achieve the best fit for the spectrum of interest in MicroAnalysis Toolkit (Supplementary Data 4).

SUPPLEMENTARY TEXT

Melanosome morphology changes during maturation.

The geometry of melanosomes from both *Xenopus* skin and liver was altered during maturation in DD water and Cu-solution (Fig. S5) (Fig. S6, Supplementary Data S5). In untreated extracts, liver melanosomes are significantly larger than skin melanosomes (Fig. S6, Supplementary Data S5 and S6). After maturation in DD water, melanosomes from the liver are significantly larger than untreated samples (+ 4% (length), +11% (width)); melanosomes from the skin show no significant difference in geometry. After maturation in Cu-solution, melanosomes from both tissues are significantly smaller than untreated melanosomes: liver melanosomes are reduced in length by 11% and width by -7%, whereas skin melanosomes are reduced in length by 8% and in width by 7% (Supplementary Data S6). Melanosomes from the two tissues retain significant differences in geometry, confirming that geometry is a useful parameter for discriminating melanosomes from different tissues even post-maturation.

Various studies have reported that melanosomes shrink by *ca.* 10–20% after maturation (Colleary et al., 2015, McNamara et al., 2013). In our study, melanosomes from both tissue types are smaller following maturation in Cu-solution and skin melanosomes are smaller following maturation in DD water. The origin of the increase in size of liver melanosomes following maturation in DD water is unclear.

REFERENCES

- Colleary, C., Dolocan, A., Gardner, J., Singh, S., Wuttke, M., Rabenstein, R., Habersetzer, J., Schaal, S., Feseha, M., and Clemens, M., 2015, Chemical, experimental, and morphological evidence for diagenetically altered melanin in exceptionally preserved fossils: *Proceedings of the National Academy of Sciences*, v. 112, no. 41, p. 12592–12597.
- McNamara, M. E., Briggs, D. E., Orr, P. J., Field, D. J., and Wang, Z., 2013, Experimental maturation of feathers: implications for reconstructions of fossil feather colour: *Biology Letters*, v. 9, no. 3, p. 20130184.
- Solé, V., Papillon, E., Cotte, M., Walter, P., and Susini, J., 2007, A multiplatform code for the analysis of energy-dispersive X-ray fluorescence spectra: *Spectrochimica Acta Part B: Atomic Spectroscopy*, v. 62, no. 1, p. 63–68.

Supplementary figures

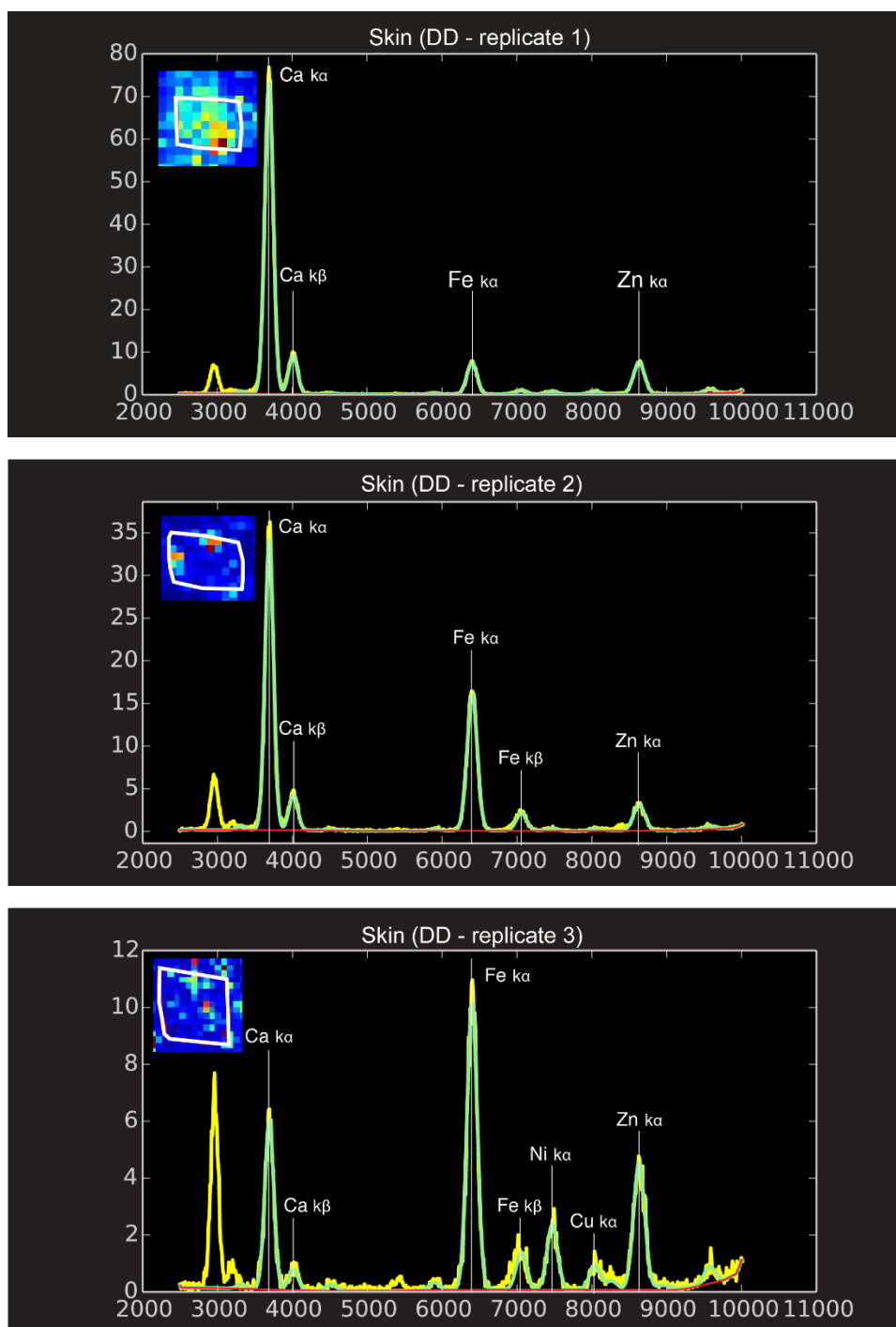


Fig S1. MCA spectra of replicates of melanosome extracts from the skin of the African clawed frog (*Xenopus laevis*) matured in distilled deionized water (DD). The X-axis represents X-ray emission energy in eV; the Y-axis represents detector counts. Yellow line represents the measured SRS-XRF spectrum; green line, the fit; red line, the continuum. Insets show region of interest in the XRF map for each replicate.

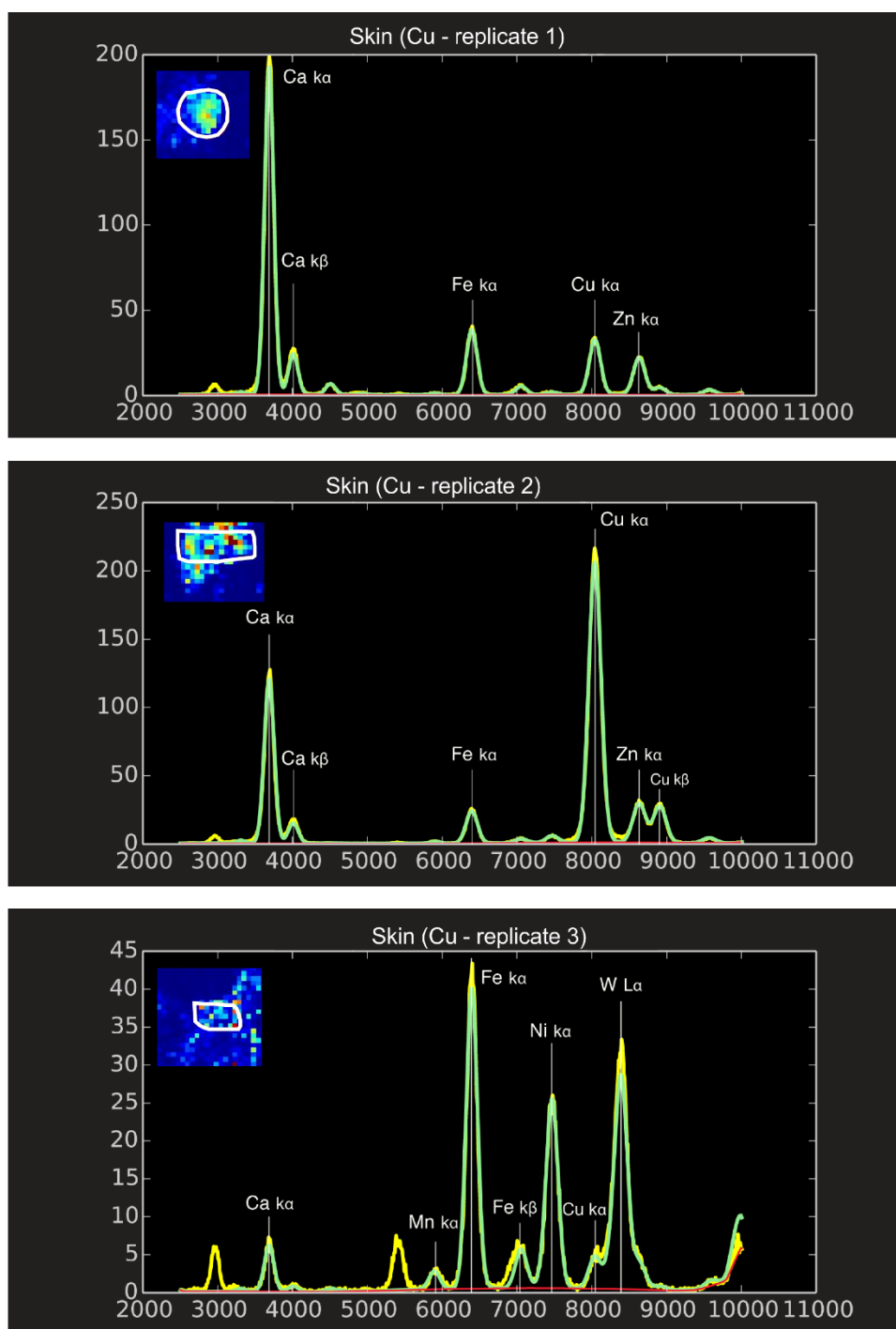


Fig S2. MCA spectra of replicates of melanosome extracts from the skin of the African clawed frog (*Xenopus laevis*) matured in Cu-solution. The X-axis represents X-ray emission energy in eV; the Y-axis represents detector counts. Yellow line represents the measured SRS-XRF spectrum; green line, the fit; red line, the continuum. Insets show region of interest in the XRF map for each replicate.

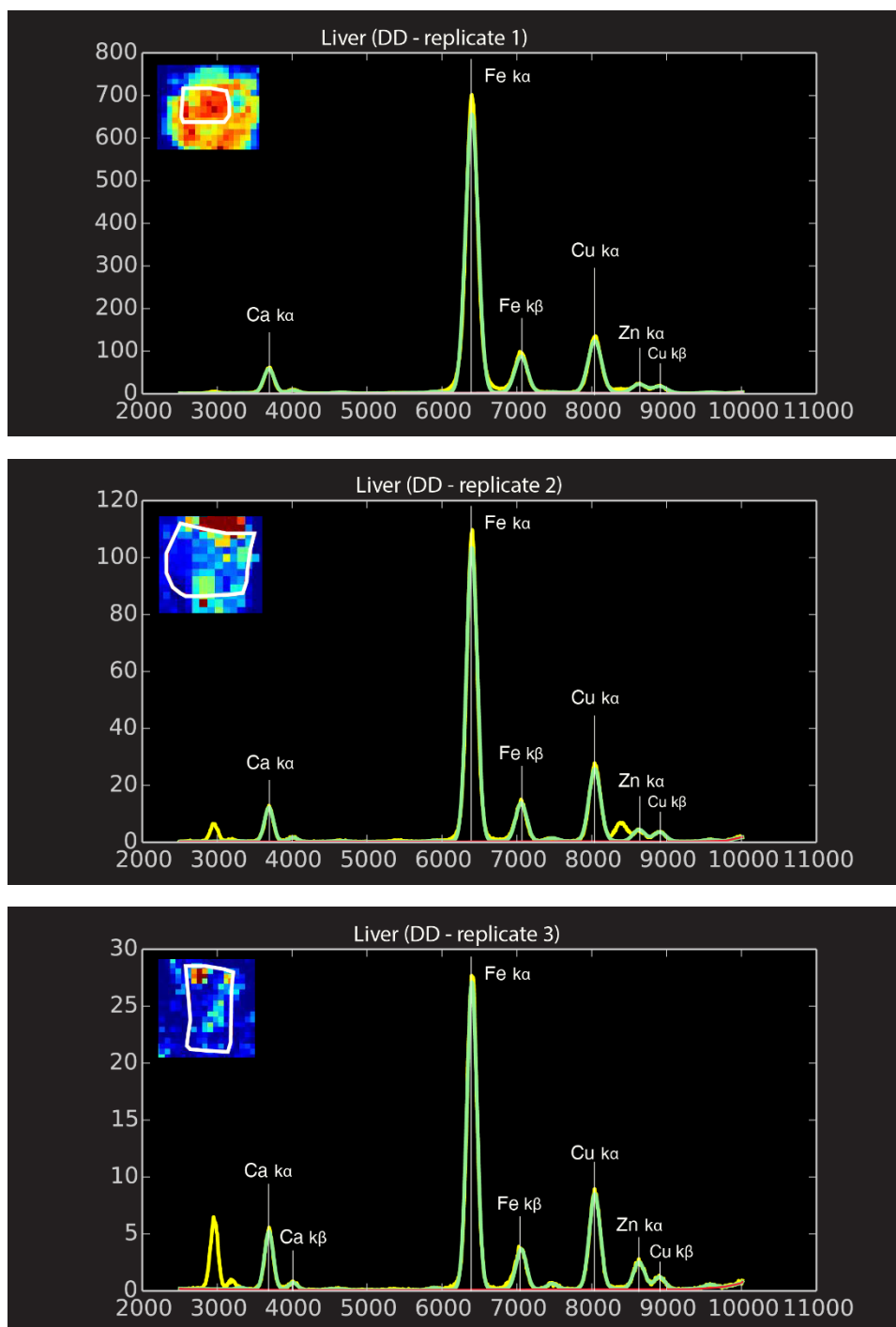


Fig S3. MCA spectra of replicates of melanosome extracts from the liver of the African clawed frog (*Xenopus laevis*) matured in distilled deionized water (DD). The X-axis represents X-ray emission energy in eV; the Y-axis represents detector counts. Yellow line represents the measured SRS-XRF spectrum; green line, the fit; red line, the continuum. Insets show region of interest in the XRF map for each replicate.

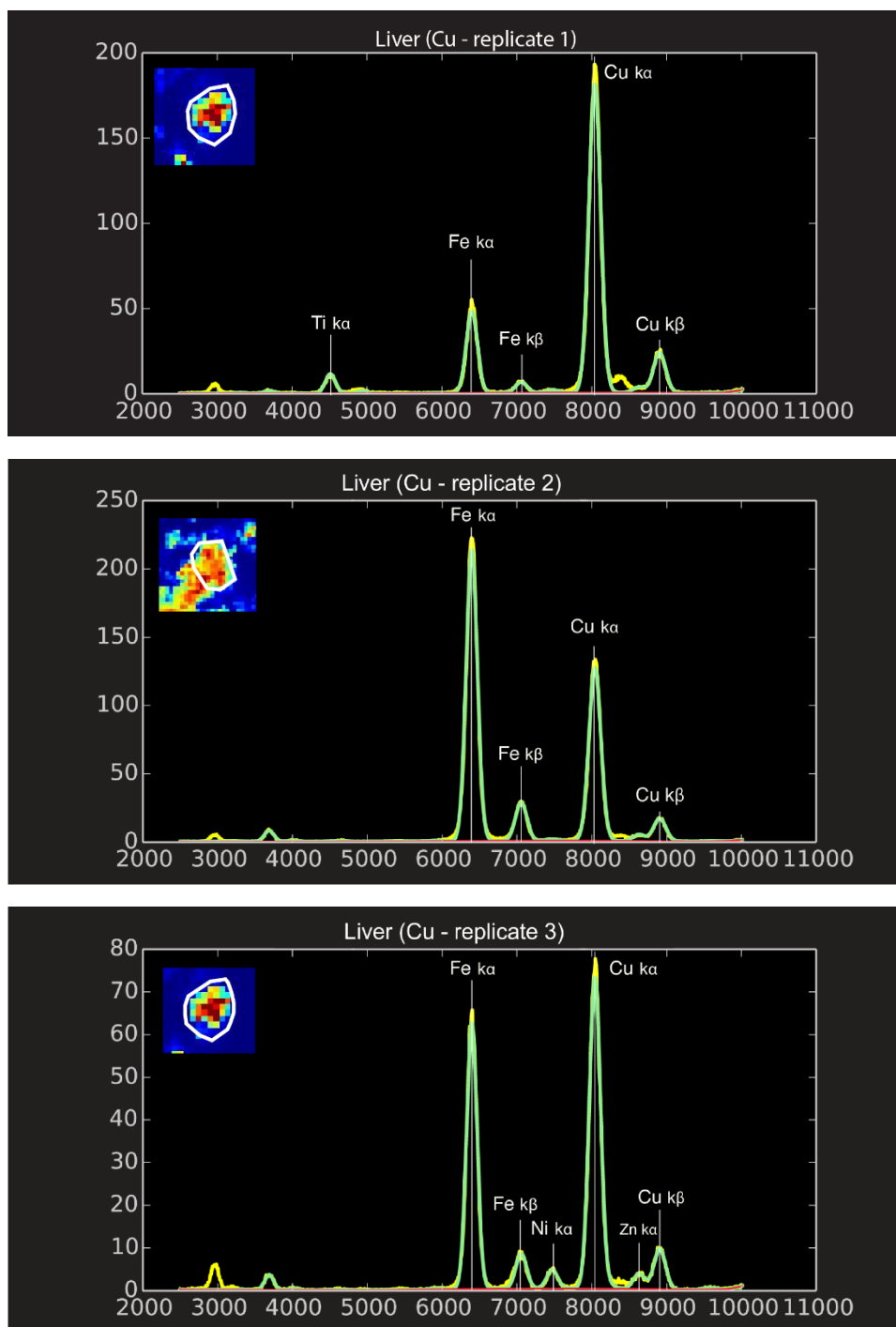


Fig S4. MCA spectra of replicates of melanosome extracts from the liver of the African clawed frog (*Xenopus laevis*) matured in Cu-solution. The X-axis represents X-ray emission energy in eV; the Y-axis represents detector counts. Yellow line represents the measured SRS-XRF spectrum; green line, the fit; red line, the continuum. Insets show region of interest in the XRF map for each replicate.

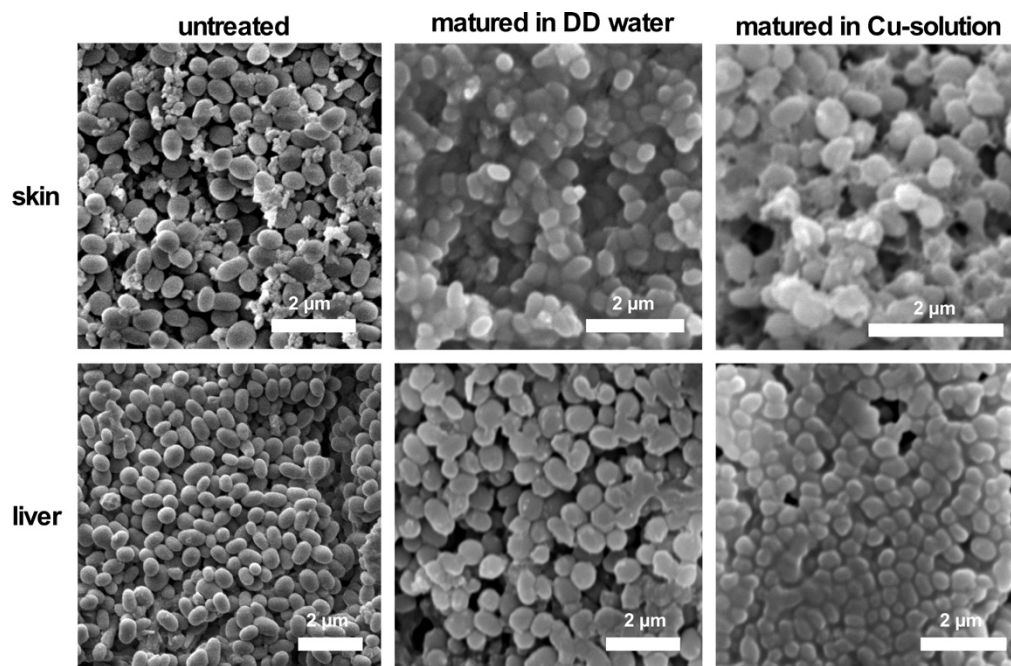


Fig S5. Scanning electron micrographs of untreated and matured melanosomes from the skin and liver of the African clawed frog (*Xenopus laevis*).

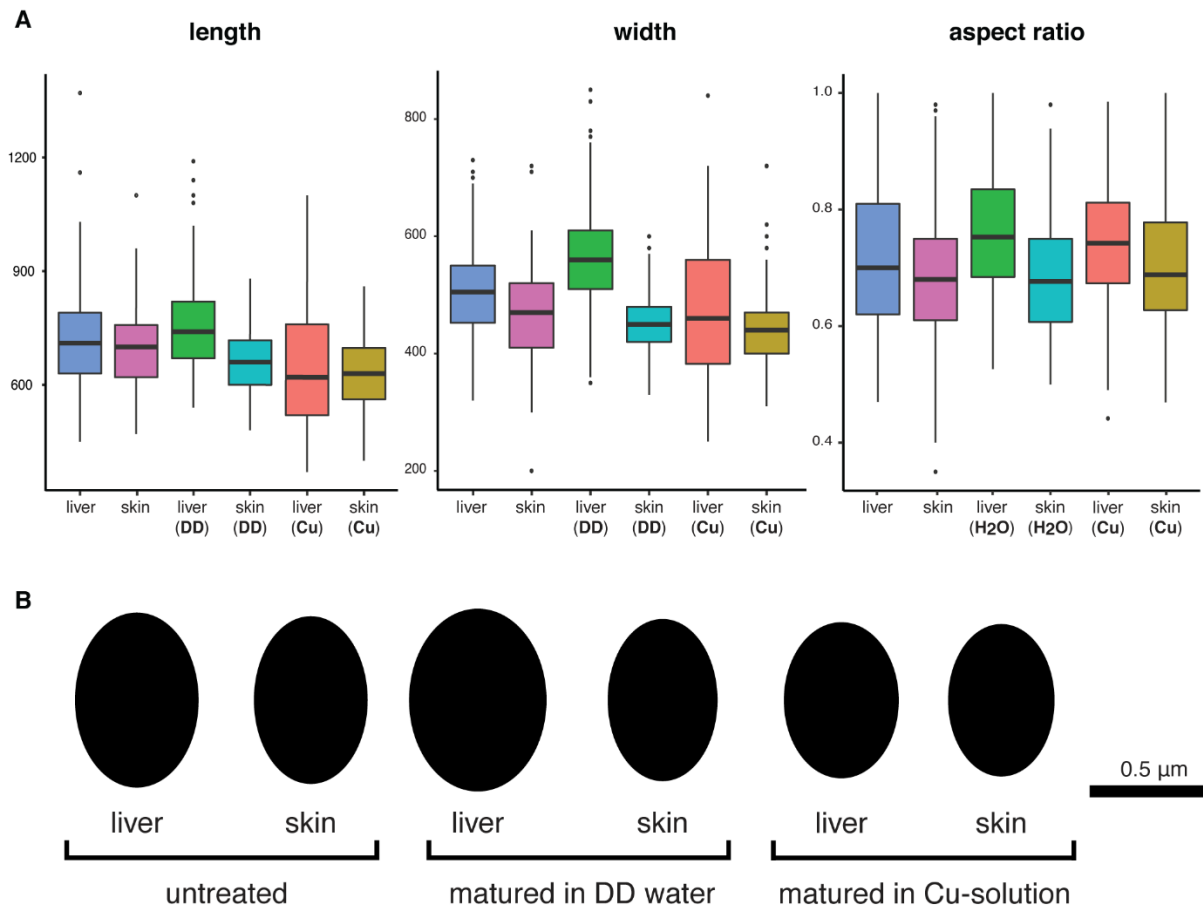


Fig. S6. Melanosome geometry and size. (A) Box plots of length, width and aspect ratio of untreated melanosomes and melanosomes matured in Cu-solution (Cu) and distilled deionized water (DD). (B) Schematic representation of melanosome morphologies before and after maturation.